# Spectral brain signatures of aesthetic natural perception in the alpha and beta frequency bands

Daniel Kaiser

*Mathematical Institute, Department of Mathematics and Computer Science, Physics, Geography, Justus-Liebig-University Gießen, Germany*
*Center for Mind, Brain and Behavior (CMBB), Philipps-University Marburg and Justus-Liebig-University Gießen, Germany*

**Correspondence**

Prof. Dr. Daniel Kaiser
Mathematical Institute
Justus-Liebig-University Gießen
Arndtstraße 2
35392 Gießen
Germany
danielkaiser.net@gmail.com
www.danielkaiser.net

**Abstract**

During our everyday lives, visual beauty is often conveyed by sustained and dynamic visual stimulation, such as when we walk through an enchanted forest or watch our pets playing. Here, I devised an MEG experiment that mimics such situations: Participants viewed 8s videos of everyday situations and rated their beauty. Using multivariate analysis, I linked aesthetic ratings to (1) sustained MEG broadband responses and (2) spectral MEG responses in the alpha and beta frequency bands. These effects were not accounted for by a set of high- and low-level visual descriptors of the videos, suggesting that they are genuinely related to aesthetic perception. My findings provide a first characterization of spectral brain signatures linked to aesthetic experiences in the real world.

## Introduction

During our everyday lives, we often encounter beauty in our visual surroundings. Such experiences are not exclusive to stimuli designed to evoke beauty, like artworks or architecture; beauty can also be found in seemingly mundane everyday experiences, like enjoying nature or observing animals. What happens in our brains during such experiences?

Research in neuroaesthetics has made great progress by studying responses to static naturalistic images, such as pictures of faces [1-3] and scenes [4-6]. However, recent investigations suggest that dynamic, compared to static, visual stimuli can evoke stronger feelings of beauty and greater task engagement [7].

So far, only few studies focused on such dynamic aesthetic experiences. A recent fMRI study [8] showed that beautiful dynamic scenes activate the hippocampus more strongly than beautiful static scenes. Another study reported activation changes in the default-mode and fronto-parietal attention networks when participants watched awe-inducing videos [9]. Interestingly, Isik and Vessel [10] showed that the beauty of dynamic visual landscapes is represented in regions distinct from regions activated by static landscapes [6], suggesting that dynamic aesthetic experiences lead to distinctive brain dynamics.

One possibility is that dynamically evolving natural stimuli give rise to unique spectral brain signatures. Our brains exchange information across regional neural assemblies through oscillatory codes [11,12], where brain regions couple or de-couple as a function of external inputs and cognitive states. Studying sustained aesthetic experiences with dynamic stimuli provides a unique opportunity for uncovering how spectral responses relate to aesthetic perception.

Here, I tested whether aesthetic experiences from rich and dynamic natural stimuli are indeed accompanied by characteristic spectral brain dynamics. Using multivariate analyses of MEG data, I found that neural activations in the alpha and beta frequency range predicted participants' ratings, providing a spectral brain signature for aesthetic perception in dynamic real-world context.

## Results

I recorded MEG while 20 participants viewed 8-second videoclips of everyday situations and rated how aesthetically pleasing or, in other words, how beautiful they found each of the videos (Figure 1a/b). Details are reported in Materials and Methods.

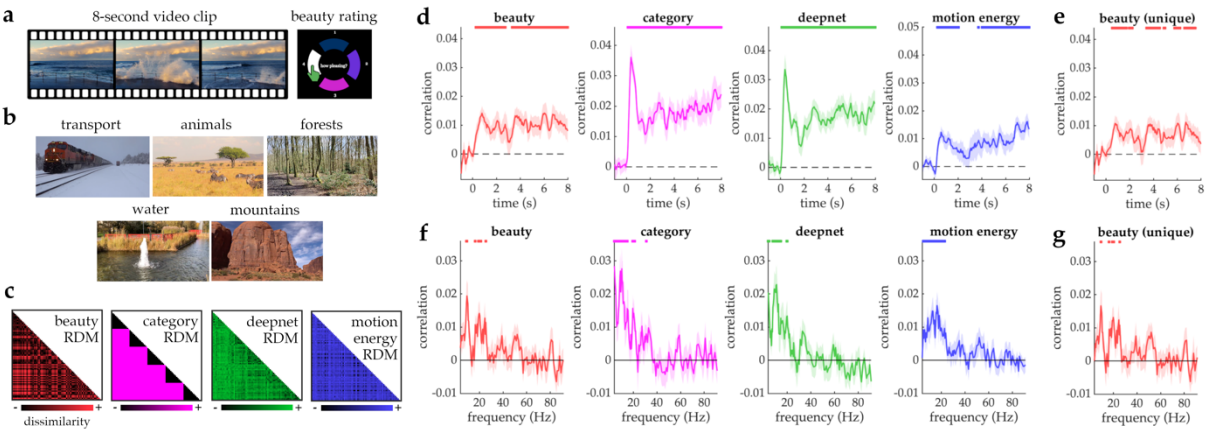


***Figure 1. a)*** *Illustration of the rating paradigm.* ***b)*** *Examples from the 5 video categories.* ***c)*** *Neural similarities (across time or frequency) were modelled with similarities in beauty ratings, category, deepnet features, and motion energy.* ***d)*** *Correlations between broadband responses and representational models.* ***e)*** *Correlation between broadband responses and beauty ratings when the other predictors are partialed out.* ***f/g)*** *Correlations between spectral responses and representational models. Error bars represent SEM. Significance markers denote* $p_{corr}<0.05$.

To quantify the neural correlates of aesthetic perception, I computed pairwise neural distances between all videos used in the experiment in a representational similarity analysis (RSA). First, I computed similarities between videos from correlations of evoked broadband responses across MEG sensors, in steps of 50ms (see Materials and Methods). I then modelled these neural distances with a predictor that captured how similar the videos were rated by the participants (Figure 1c). This analysis revealed sustained representation of aesthetic quality across the whole video presentation, starting from 250-300ms (peak at 6,000-6,050ms) (Figure 1d). To unequivocally attribute these effects to differences in aesthetic perception, I devised a set of three control predictors, which captured (i) whether the videos belonged to the same or to different visual categories, (ii) how similar the videos were in the high-level features extracted by the final layer of deepnet trained on scene categorization, and (iii) how similar the videos were in their spatiotemporal energy in low-level visual features (Figure 1c; see Materials and Methods). These control predictors also reliably correlated with neural representations (Figure 1d). When partialing out the control

predictors, however, aesthetic quality ratings still predicted neural responses in a reliable fashion from 500-550ms (peak at 6,700-6,750ms) (Figure 1e).

To unveil the spectral correlates of aesthetic perception, I performed an RSA on trial-wise powerspectra extracted from ongoing activity during the video presentation (see Materials and Methods). Pairwise similarities between videos were constructed from correlations between power values across all MEG sensors, separately for each frequency. I then again modelled these using the four predictors used above. Ratings of aesthetic quality were reliably associated with spectral features in the alpha (9-9.5Hz, peak at 9.5Hz) and beta (16.5Hz, 19-21Hz, 25.5Hz, peak at 20Hz) frequency bands (Figure 1g), also when partialing out the control predictors (alpha: single peak at 9.5Hz; beta: 16.5Hz, 19-20.5Hz, 25.5Hz, peak at 20Hz) (Figure 1f). Similar results were obtained when excluding the first 2s of processing, omitting the initial visual response (see SI). This result establishes a spectral neural signature of aesthetic perception of natural and dynamic visual inputs in the alpha/beta frequency range.

**Discussion**

The current results demonstrate that the aesthetic appeal of dynamic natural videos is not only encoded in sustained broadband responses, but also in spectral activations in the alpha and beta frequency range. Control analyses further suggest that the spectral coding of aesthetic appeal is independent of scene category, complex deepnet features, and low-level motion energy. These findings provide a spectral signature of aesthetic perception under ecologically valid conditions – that is, during the dynamic visual experiences we encounter in real life.

Two previous studies have looked at spectral neural correlates of aesthetic perception with static images. First, consistently with our study, Kang and colleagues [2] reported an association between facial beauty and EEG alpha activity. Second, Strijbosch and colleagues [13] reported that gamma activity differentiated between aesthetically moving and non-moving art, while beta activity differentiated between moderately and highly moving art. My results are consistent with the low-frequency effects reported in this study. The absence of gamma-band differences here may be related to the longer presentation times or the everyday videos not spanning a sufficient range of beauty ratings.

A possible explanation for the beauty-related alpha/beta activations is their putative role in top-down processing [12]: Under conditions of sustained real-world experiences, it is likely that top-down modulations, caused by cognitive evaluations [14], play a major role in determining aesthetic appeal. Though largely speculative at this point, this assertion could be tested in future studies combining time-resolved M/EEG with spatially resolved fMRI.

Together, the current study provides an important starting point for further consideration of spectral signal components in visual neuroaesthetics.

**Materials and Methods**

*Participants.* Twenty adult volunteers with normal vision participated (mean age 24.2, SD=7.0; 16 female, 4 male). They received monetary reimbursement or course credits. Sample size was constrained by scan time availability. All participants provided written informed consent. Procedures were approved by the Research Ethics Committee of the York Neuroimaging Centre and adhered to the Declaration of Helsinki.

*Stimuli and Paradigm.* Stimuli were 75 8s-videos (1280×720, 30Hz) of everyday events, spanning five categories (15 each): transport, animals, forests, water, mountains. A list of descriptions can be found in SI. In each of four runs (~15min each), all videos (17×9.6deg visual angle) were shown in random order. For an analysis across categories, see SI. Participants were instructed to maintain fixation and rate how aesthetically pleasing, or beautiful, they found the video using a 4-level circular rating scale. The position of response options varied (always increasing clockwise) to disentangle ratings from motor responses.

*MEG recording and processing.* MEG was recorded at 1000 Hz using a 248-channel 4D Neuroimaging Magnes3600 system. Data were downsampled to 200Hz, epoched from -1s to 9s relative to onset, and baseline-corrected [15]. Noisy channels were removed and interpolated using neighboring channels. Eye and heart artifacts were removed using ICA.

*Spectral responses.* For computing spectral responses, I split every trial into 4 bins of 2 seconds (0-2s, 2-4s, 4-6s, 6-8s), which were treated as individual samples. For each

channel and sample, powerspectra were obtained from DPSS multitaper analyses [15] with spectral smoothing of ±3Hz (4-30Hz) or ±6Hz (31-91Hz). Power values were computed in 0.5Hz-steps (4-30Hz) or 1Hz-steps (31-91Hz) and converted to dB.

*Representational similarity analysis.* Neural representational dissimilarity matrices (RDMs) were created from broadband responses (across time) or spectral responses (across frequencies). Half of the data was used to reduce data dimensionality using PCA, and the other half was used to correlate response patterns to obtain an index of pairwise dissimilarity [1,4]. RDMs were corelated with predictor RDMs that captured the videos' similarity in: (i) beauty ratings, (ii) category, (iii) high-level deepnet features, and (iv) low-level motion energy. A detailed description can be found in SI.

*Statistical testing.* One-sided t-tests were used to compare correlations against zero. P-values were FDR-corrected for multiple comparisons; only effects with $p_{corr}<0.05$ are reported.

*Data sharing*. Data will be made available on OSF upon publication.

**Acknowledgements**

MEG data was acquired at the York Neuroimaging Centre. Thanks to Richard Aveyard for help with MEG setup and acquisition. D.K. is supported by the DFG (INST162/567-1) and "The Adaptive Mind", funded by the Excellence Program of the Hessian Ministry of Higher Education, Science, Research and Art. No conflicts of interest are declared.

**References**

[1] Kaiser, D., & Nyga, K. (2020). Tracking cortical representations of facial attractiveness using time-resolved representational similarity analysis. *Scientific Reports*, *10*(1), 1-10.

[2] Kang, J. H., Kim, S. J., Cho, Y. S., & Kim, S. P. (2015). Modulation of alpha oscillations in the human EEG with facial preference. *PloS one*, *10*(9), e0138153.

[3] Winston, J. S., O'Doherty, J., Kilner, J. M., Perrett, D. I., & Dolan, R. J. (2007). Brain systems for assessing facial attractiveness. *Neuropsychologia*, *45*(1), 195-206.

[4] Kaiser, D. (2022). Characterizing dynamic neural representations of scene attractiveness. *J Cogn Neurosci*. doi.org/10.1162/jocn_a_01891

[5] Kawabata, H., & Zeki, S. (2004). Neural correlates of beauty. *Journal of Neurophysiology*, *91*(4), 1699-1705.

[6] Vessel, E. A., Isik, A. I., Belfi, A. M., Stahl, J. L., & Starr, G. G. (2019). The default-mode network represents aesthetic appeal that generalizes across visual domains. *Proceedings of the National Academy of Sciences*, *116*(38), 19155-19164.

[7] Welke, D., & Vessel, E. A. (2022). Naturalistic viewing conditions can increase task engagement and aesthetic preference but have only minimal impact on EEG quality. *NeuroImage*, *256*, 119218.

[8] Zhao, X., Wang, J., Li, J., Luo, G., Li, T., Chatterjee, A., ... & He, X. (2020). The neural mechanism of aesthetic judgments of dynamic landscapes: an fMRI study. *Scientific Reports*, *10*(1), 1-11.

[9] Van Elk, M., Arciniegas Gomez, M. A., van der Zwaag, W., Van Schie, H. T., & Sauter, D. (2019). The neural correlates of the awe experience: Reduced default mode network activity during feelings of awe. *Human Brain Mapping*, *40*(12), 3561-3574.

[10] Isik, A. I., & Vessel, E. A. (2021). From visual perception to aesthetic appeal: Brain responses to aesthetically appealing natural landscape movies. *Frontiers in Human Neuroscience*, 414.

[11] Buzsaki, G., & Draguhn, A. (2004). Neuronal oscillations in cortical networks. *Science*, *304*(5679), 1926-1929.

[12] Fries, P. (2015). Rhythms for cognition: communication through coherence. *Neuron*, *88*(1), 220-235.

[13] Strijbosch, W., Vessel, E. A., Welke, D., Mitas, O., Gelissen, J., & Bastiaansen, M. (2022). On the neuronal dynamics of aesthetic experience: Evidence from electroencephalographic oscillatory dynamics. *Journal of Cognitive Neuroscience*, *34*(3), 461-479.

[14] Leder, H., Belke, B., Oeberst, A., & Augustin, D. (2004). A model of aesthetic appreciation and aesthetic judgments. *British Journal of Psychology*, *95*(4), 489-508.

[15] Oostenveld, R., Fries, P., Maris, E., & Schoffelen, J. M. (2011). FieldTrip: open source software for advanced analysis of MEG, EEG, and invasive electrophysiological data. *Computational Intelligence and Neuroscience*, *2011*.

**Supplementary Information (SI)**

*Representational similarity analysis details*

Neural RDMs were created in an analogous way to our previous studies on face and scene attractiveness [1,4], using the CoSMoMVPA toolbox for Matlab [16]. For the broadband responses, analysis was done separately for consecutive time-bins of 50ms, where all raw data falling into each time bin was used as a composite response pattern across sensors and time. For the spectral responses, analyses were done separately for each frequency step. The data of each participant was repeatedly split into two halves (each possible 50/50 split of the four runs). The first half of the data was used for dimensionality reduction of the neural response patterns [17]: The response patterns across channels was subjected to a PCA and the components explaining 99% of the variance were retained. The PCA solution was projected onto the second half of the data. The second half of the data was then used to compute neural dissimilarity: The response patterns were correlated (Spearman-correlations) across all possible pairs of videos, yielding a 75×75 neural RDM for each timepoint (in the analysis of broadband responses) or each frequency (in the analysis of spectral responses). These neural RDMs were then correlated (Spearman-correlations) with a set of model RDMs, separately for each participant; for these correlations, only the lower off-diagonal entries of the matrices were used.

I devised four model RDMs. First, I created an RDM that reflected the videos' pairwise dissimilarities in beauty ratings. For this RDM, the absolute difference between each participants' own beauty ratings (averaged across the four repetitions) was computed for each pair of videos. Each participant's neural data was thus modelled using their own beauty ratings. Second, I created an RDM that reflected the videos' pairwise dissimilarities in category. For this RDM, scenes from the same category (e.g., two videos depicting animals) were coded as similar (0) and two videos from different categories were coded as dissimilar (1). Third, I created an RDM that reflected the videos' pairwise dissimilarities in high-level features extracted by a GoogLeNet deep neural network [18] trained on scene categorization using the Places365 image set [19]. For this RDM, activations were extracted from the last layer of the DNN and correlated for each pair of images; correlations were then subtracted from 1. Fourth, I created an RDM that reflected the videos' pairwise dissimilarities in low-level visual motion energy measured by a wavelet-pyramid-based model [20]. For this, model activations

were extracted and correlated across each pair of videos; correlations were then subtracted from 1.

For the control analyses, I re-computed the correlations of the neural RDMs and the model RDM based on beauty ratings while partialing out (using partial Spearman-correlations) the model RDMs based on category, deepnet features, and motion energy.

For the broadband responses, all correlations between the neural RDMs and model RDMs were smoothed with a running average of 5 time points (i.e., 250ms), separately for each participant.

*Spectral responses after the initial visual response*

To assess whether the spectral signatures of aesthetic perception obtained previously were due to the frequencies contained in the visual response evoked by the video onset, we conducted an analyses in which we only used the data segments from 2-4s, 4-6s, and 6-8s. The analyses details were otherwise identical. This analysis revealed significant correspondences between the beauty ratings and neural representations in the alpha (8-10.5Hz, 12Hz, peak at 9.5Hz) and beta bands (16-17.5Hz, 19-20.5Hz, 24-24.5Hz, 25.5Hz). A similar result was obtained when partialing out the control predictors (alpha: single peak at 9.5Hz; beta: 16.5-17Hz, 19.5Hz, 20.5Hz, 24-24.5Hz, peak at 24.5Hz). This shows that the spectral alpha/beta signature obtained previously (Figure 1e/g) is not solely explained by frequencies contained in the initial evoked response.

*Beauty ratings across categories*

Analyzing the beauty ratings across categories, I found that ratings differed across categories ($F[4,76]=4.35$, $p<0.001$). The following means and standard errors were observed (1: worst rating, 4: best rating): transport M=1.81, SE=0.10; animals M=2.56, SE=0.08; forests M=2.82, SE=0.09; water M=3.01, SE=0.06; mountains M=2.78, SE=0.06. To test whether these differences between categories account for the neural correlates of aesthetic ratings, I performed an analysis where I correlated the neural RDMs with the RDM based on beauty ratings while partialing out a predictor RDM that reflected the categories' absolute differences in mean ratings. For the broadband responses, I

still obtained a significant correlation that was highly similar to the previous results (Figure 1d/e), subtending large parts of the epoch from 500-550ms (peak at 6,000-6,050ms). For the spectral responses, I again found correspondences in the alpha (single peak at 9.5Hz) and beta (16.5Hz, 17.5Hz-18Hz, 19-21Hz, 25.5Hz, peak at 20Hz) bands. This shows that the effects cannot be accounted for by rating differences between categories.

*Video descriptions*

Transport:

(1) A steam train arriving on a railway platform
(2) An Airbus A380 airplane landing on an airport runway
(3) A cable car crossing a bridge
(4) A view around a motorbike on a field
(5) A view around a pickup truck on a parking lot
(6) A freight train passing by in a wintery landscape
(7) A freight train passing a railway station
(8) A Concorde airplane taking off at sunset
(9) A train ploughing through heavy snow
(10) An airplane taxiing along the airport
(11) Heavy car traffic at a roundabout around a statue
(12) An aerial view of traffic at a motorway toll station
(13) An icebreaker ship crossing pack ice
(14) An aerial view of motorway traffic
(15) Military trucks driving along a road

Animals:

(16) Two dogs playing on the beach
(17) A bird eating a breadcrumb
(18) A sloth hanging from a tree
(19) A peacock walking on a city terrace
(20) A group of camels relaxing in the desert sand
(21) A group of monkeys playing on the grass
(22) Two elephants eating grain
(23) Zebras grazing on a prairie
(24) Two dogs playing in front of a house
(25) A group of lions walking across a prairie

(26) A horse drinking water on a muddy road
(27) Horses eating grass on a field in the mountains
(28) Dogs playing in a park
(29) A cat roaming around a strip of concrete in a garden
(30) Caterpillars eating a leaf

Forests:

(31) A view across a sunlit forest
(32) A view across a forest meadow
(33) First-person perspective of a walk along a street surrounded by trees
(34) Twigs shaking in the wind
(35) A view across a park
(36) Grass on a forest meadow shaking in the wind
(37) Rain falling on flowers in a forest
(38) A view across forest soil and mushrooms
(39) Large trees shaking in the wind
(40) First-person perspective of a walk along a forest path
(41) First-person perspective of a walk through the forest
(42) Flowers on a field in front of a forest
(43) View across a sunlit forest in autumn
(44) Mushrooms and grass shaking in the wind
(45) First-person perspective of a walk along a forest path in autumn

Water:

(46) Aerial view of waves crashing on a rocky island
(47) A water fountain in a park
(48) Aerial view of a waterfall at a cliff
(49) First-person view of a fishing rod hovering over shallow waters
(50) Waves crashing on a shorefront promenade
(51) Water flowing along a shallow creek
(52) A waterfall in the mountains
(53) Water flowing down a rocky mountain
(54) A view of a small lake in autumn
(55) A small river flowing in a forest
(56) Waves moving at open sea
(57) An aerial view of a cliff with waves crashing
(58) A view across a lake in a park
(59) A waterfall flowing from a cliff into a small lake

(60) Small waves flowing onto a beach

Mountains:

(61) Aerial view across a misty valley in the evening
(62) View across red rock formations in the desert
(63) Aerial view of a snow-covered mountain peak
(64) Fog rising between mountains
(65) View of a set of weirdly shaped rock formations
(66) View of a snow-covered field on a mountain
(67) Flowers moving in the wind in front of a mountain scenery
(68) View across mountains and caves in the desert
(69) View across plains in front of snow-covered mountains
(70) View from a mountaintop down a rocky valley
(71) View across red rock formations
(72) View across a mountain wall with small caves
(73) View across man-made caves in a mountain
(74) Aerial view of a rocky valley
(75) View of mountain tops covered in fog

*Supplementary References*


[16] Oosterhof, N. N., Connolly, A. C., & Haxby, J. V. (2016). CoSMoMVPA: multi-modal multivariate pattern analysis of neuroimaging data in Matlab/GNU Octave. *Frontiers in Neuroinformatics*, *10*, 27.

[17] Grootswagers, T., Wardle, S. G., & Carlson, T. A. (2017). Decoding dynamic brain patterns from evoked responses: A tutorial on multivariate pattern analysis applied to time series neuroimaging data. *Journal of Cognitive Neuroscience*, *29*(4), 677-697.

[18] Szegedy, C., Wei, L., Jia, Y., Sermanet, P., Reed, S., Anguelov, D., … & Rabinovich, A. (2014). Going deeper with convolutions. *arXiv preprint arXiv:1409.4842*.

[19] Zhou, B., Khosla, A., Lapedriza, A., Torralba, A., & Oliva, A. (2016). Places: An image database for deep scene understanding. *arXiv preprint arXiv:1610.02055*.

[20] Nishimoto, S., Vu, A. T., Naselaris, T., Benjamini, Y., Yu, B., & Gallant, J. L. (2011). Reconstructing visual experiences from brain activity evoked by natural movies. *Current Biology*, *21*(19), 1641-1646.